Frequency-Offset Sensitivity of Resilient Microwave Links Applying the Alamouti Scheme

Jan Mietzner, Jan Eick, and Peter A. Hoeher
Information and Coding Theory Lab, Faculty of Engineering, University of Kiel, Kaiserstrasse 2, D-24143 Kiel, Germany
WWW: `www-ict.tf.uni-kiel.de` E-mail: `{jm,jei,ph}@tf.uni-kiel.de`

***Abstract*— Space-time codes were designed for fading environments in order to improve system capacity and/or to achieve a diversity gain. In this paper, a novel possible application of the Alamouti space-time block code (STBC) for two transmit antennas is investigated, to provide a switchless alternative in current resilient microwave radio links. Resilient means that transmitter (Tx) and receiver (Rx) are each equipped with two complete, independent, parallel Tx/Rx chains and particularly with two antennas. Conventionally, only one Tx/Rx chain is active, while the other one is kept in a 'hot-stand-by' mode. In the proposed alternative system design based on the Alamouti STBC, both Tx antennas are utilized at the same time. Since the Alamouti STBC is backward compatible with the single transmit antenna system, one Tx chain may fail without causing a rate loss. However, a resilient Tx/Rx structure implies that two independent local oscillators are employed for up-conversion as well as for down-conversion, i.e., the local oscillators at each antenna may independently differ from the nominal carrier frequency. It is shown here that in this case the orthogonality of the Alamouti STBC is lost, even if the frequency offsets are perfectly known at the receiver. Analytical expressions for the bit error probability as a function of the frequency offsets are derived, and the performance loss occurring in the case of perfect and non-perfect knowledge of the frequency offsets at the receiver is illustrated on the basis of simulation results.**

***Index Terms*— Wireless communications, multiple antennas, space-time codes, Alamouti scheme, microwave radio link, frequency offset.**

I. INTRODUCTION

IN WIRELESS communication systems, the application of multiple transmit (Tx) and/or multiple receive (Rx) antennas has recently gained much interest [1]. In fading environments, multiple antenna systems promise huge capacity gains over conventional (1x1)-systems with only one Tx and one Rx antenna (e.g., [2]–[4]) or – especially in rich scattering environments – large spatial diversity gains (e.g., [5]–[8]) or a trade-off of both. Spatial diversity results from the fact that the individual transmission paths from the Tx antennas to the Rx antennas are likely to fade independently, i.e., the probability that each path is degraded at the same time is significantly smaller than the probability that a single transmission path is in a deep fade.

In a multiple antenna system, signal processing is not only performed in the time domain, but also in the spatial domain, i.e., across the individual Tx and Rx antennas. *Spatial multiplexing (SM)* schemes such as the Bell Labs Layered Space-Time Architecture (BLAST) [4] employ multiple antennas at both sides of the wireless link and transmit independent data streams over the individual Tx antennas. At the receiver, the data streams are separated again by employing an interference-cancellation (IC) type of algorithm. SM schemes enhance the overall data throughput and yield a significant fraction of the promised capacity. As opposed to SM schemes, *space-time codes (STCs)* such as space-time trellis codes (STTCs) [9],[10] and space-time block codes (STBCs) [11],[12] exploit spatial diversity. This yields an additional diversity and/or coding gain compared to the (1x1)-system. By this means, an improved bit error rate performance is accomplished, which may in turn be translated to higher throughput, if an adaptive modulation/channel coding scheme is applied. With STTCs and STBCs, multiple antennas at the receiver are optional. Recently, novel schemes have been introduced that are a combination of SM and STC, e.g. [13].

In this paper, the novel possible application of STCs in *resilient* microwave radio communication links with a line-of-sight (LOS) component[1] is investigated [14]. Resilient means that transmitter and receiver are each equipped with two complete, independent, parallel Tx/Rx chains. In particular, two antennas as well as two *independent* local oscillators (LOs), employed for up/down-conversion of the transmitted/received signals, are assumed at either end of the link. Due to resilience, we do not want to couple the LOs.

Conventionally, only one Tx/Rx chain is active, while the other one is kept in a 'hot-stand-by' mode. Focus is on the wireless interconnection of base stations (BSs) or other fixed nodes within a cellular mobile radio network. Other application examples include satellite links to fixed earth stations and fixed broadband wireless access networks connecting residential sites to a high-data-rate backbone network ('last mile'). Here, an alternative resilient system design based on the Alamouti scheme[2] [15] is proposed (Section II) because of the following reasons:

- The Alamouti STBC is shown to yield significant diversity gains under realistic assumptions, when the two Tx antennas are simultaneously active (Section III).
- The data rate of the conventional (1x1)-system is retained.
- Since the Alamouti STBC is backward compatible with the (1x1)-system, one Tx chain may fail without causing a rate loss. Therefore, the proposed system based on the Alamouti STBC is resilient as well.
- The Alamouti STBC does virtually not affect the complexity of the transmitter or the receiver.
- Optionally, both antennas available at the receiver may be utilized simultaneously.

Since two independent LOs are employed at each Tx antenna – due to the resilient Tx structure, two different frequency offsets typically occur in the transmitter, because the LOs may independently differ from the nominal carrier frequency. The same

[1] It was already shown in [9] that STCs yield considerable diversity gains, even if there is a strong LOS component.

[2] The Alamouti scheme is the simplest special case of an orthogonal STBC and employs two transmit antennas.

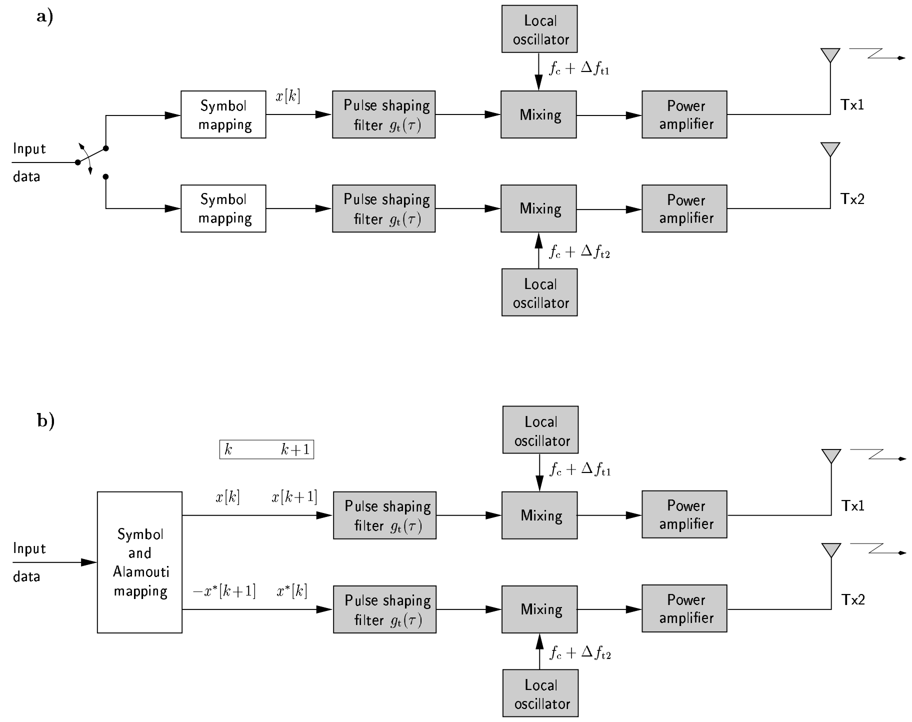

Fig. 1. Comparison between the transmitter structure a) of the conventional system and b) of the proposed system design based on the Alamouti STBC. Components subject to possible failures are highlighted by gray color.

is true for the LOs in the receiver.

The same problem may occur, when *distributed* space-time processing is applied, for example in relay-assisted wireless networks, where several single-antenna relay nodes forwarding the same information cooperate in a STC scheme, in order to achieve a diversity gain [16].

The influence of the frequency offsets is investigated in Section IV. It is shown that the orthogonality of the Alamouti STBC is lost, even if a modified receiver is used having *perfect* knowledge of all involved frequency offsets. In Section V, analytical expressions for the bit error probability as a function of the frequency offsets are derived for the example of quaternary phase-shift keying (QPSK). On the basis of simulation results for a Rician fading channel, the performance loss which occurs in the case of perfect and non-perfect knowledge of the frequency offsets at the receiver is illustrated (Section VI).

II. Proposed System Design

In the following, the proposed resilient system design based on the Alamouti STBC is presented. Throughout this paper, the equivalent complex baseband representation is used.

In the Alamouti STBC, M-ary data symbols are processed as pairs $[\,x[k], x[k+1]\,]$ and are transmitted over two antennas according to

$$\begin{array}{c} \mathbf{A} \doteq \left[\begin{array}{cc} x[k] & -x^*[k+1] \\ x[k+1] & x^*[k] \end{array} \right] \begin{array}{l} \longleftarrow \text{Time index } k \\ \longleftarrow \text{Time index } k+1 \end{array} \\ \begin{array}{cc} \uparrow & \uparrow \\ \text{Ant. 1} & \text{Ant. 2} \end{array} \end{array} \quad (1)$$

where $(.)^*$ denotes complex conjugation[3]. The Alamouti matrix $\mathbf{A}$ is orthogonal and $\mathbf{A}^{\mathrm{H}}\mathbf{A} = (|x[k]|^2 + |x[k+1]|^2)\,\mathbf{I}_2$, where $\mathbf{A}^{\mathrm{H}}$ is the hermitian conjugate of $\mathbf{A}$ and $\mathbf{I}_2$ the (2×2)-identity matrix. In the case of a frequency-flat fading channel, this property enables maximum-ratio combining (MRC) by means of a simple matrix multiplication (see Section IV), provided that the channel is perfectly known at the receiver [15].

In Fig. 1, the transmitter structure of the conventional system is compared with the one of the proposed alternative system design based on the Alamouti STBC. As can be seen from Fig. 1, the conventional system uses only one Tx chain at a time. As opposed to this, the system design based on the Alamouti STBC utilizes both Tx chains simultaneously. First, symbol mapping and Alamouti mapping is performed. Subsequently, pulse shaping is applied (square-root Nyquist filter $g_{\mathrm{t}}(\tau)$). Finally, the baseband signals are converted to passband and the resulting RF signals are amplified and transmitted over the two Tx antennas. It is assumed that the LOs employed to up-convert the two transmission signals introduce frequency offsets Δf_{t1} (antenna Tx1) and Δf_{t2} (antenna Tx2) with respect to the nominal carrier frequency f_{c}. Note that the step from the conventional system to the proposed system does not require substantial modifications of the hardware.

At the receiver, one or two Rx antennas may be used. The received RF signal(s) are converted to baseband, where a frequency offset $\Delta f_{\mathrm{r1}}, \Delta f_{\mathrm{r2}}$ is assumed for the first and the second Rx antenna. Then, matched filtering and sampling is performed and finally Alamouti detection and symbol demapping.

[3]In this paper, the transposed of the original matrix [15] is used.

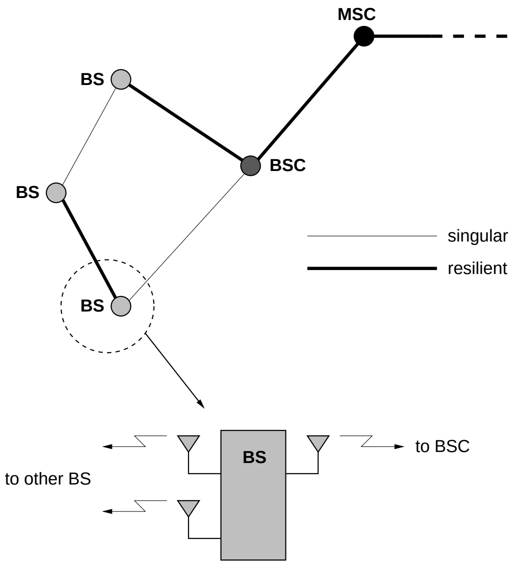

Fig. 2. Example for a resilient point-to-point link between two BSs within a cellular mobile radio network.

III. Application Example: Wireless Interconnection of Base Stations

In many cellular mobile radio networks, microwave radio links are used in order to interconnect BSs or other fixed nodes within the network, like base station controllers (BSCs) or mobile switching centers (MSCs). Such point-to-point microwave radio links are especially useful in rural areas, where the average distance between two nodes tends to be quite large. By implementing resilient links, maintenance of particularly important links may be granted with a high probability. An example for a resilient link between two BSs within a cellular network [17] is given in Fig. 2.

A. Link Model and Channel Model

Based on realistic assumptions, a link model and a channel model is developed in [14] for a point-to-point microwave radio link between two BSs situated in a rural area. For detailed information concerning system parameters and assumptions made, see [14].

The link model comprises an LOS component and a scattered component, in which all rays reflected from the earth's surface are combined [18, Ch. 5.4]. The amplitude of the scattered component is assumed to be Rayleigh-distributed. Apart from the earth's surface, no other scatterers are taken into account.

The equivalent discrete-time channel model is determined by just two characteristic parameters. The first parameter is a delay τ_{d} of the scattered component with respect to the LOS component (due to the path length difference). The second parameter is the Rice factor $K \doteq P_{\mathrm{LOS}}/P_{\mathrm{refl}}$, where P_{LOS} and P_{refl} are the average received powers of the LOS component and the scattered component, respectively. In the case of a small horizontal distance between the two BSs, the path length difference is comparably large and thus is τ_{d}. At the same time, the scattered component is strongly attenuated. The converse applies if the horizontal distance is large. For realistic system parameters and dry conditions, one obtains the following values for the delay τ_{d} and the Rice factor K:

- 'Short distance scenario' (horizontal distance 500 m): $\tau_{\mathrm{d}} \approx 0.1\,T,\;\; K \approx 67$ dB,
- 'Long distance scenario' (horizontal distance 30 km): $\tau_{\mathrm{d}} \approx 0.002\,T, K \approx 0$ dB,

where T denotes the symbol duration, which is assumed to be $0.05\,\mu$s. In the short distance scenario, the channel is an additive white Gaussian noise (AWGN) channel, due to the large value of K. However, in the long distance scenario, the channel is virtually a frequency-flat Rician fading channel (due to the small delay τ_{d}) with a strong Rayleigh component. It appears that for data rates of practical interest, the channel is approximately flat for all horizontal distances, since either τ_{d} is small or the scattered component is strongly attenuated [14].

B. Diversity Gains Under Realistic Assumptions

The following simulation results illustrate the performance improvements obtainable by means of the Alamouti scheme for the above application example. The simulation results were obtained by means of Monte-Carlo simulations over 10^6 blocks, where each block contained 100 QPSK symbols ($M = 4$, Gray mapping used). Channel coding was not performed. An outer channel code may, however, be added to further improve performance. For the scattered component, quasi-static fading was assumed, i.e., the channel is constant over a complete block and changes randomly from one block to the next. The individual links between the Tx and Rx antennas were considered statistically independent. The channel coefficients were perfectly known at the receiver.

Fig. 3 presents simulation results for the long distance scenario, which is the crucial scenario in practice. Moreover, analytical curves are included [19, Ch. 14.4] for *diversity reception* of uncoded QPSK over ν statistically independent Rayleigh fading channels with identical average signal-to-noise ratios (SNRs) of $(E_s/N_0)/\nu$ (N_0 denotes the single-sided noise power density and E_s the average energy per data symbol). In all cases, E_s/N_0 is normalized w.r.t. the number of Tx and Rx antennas. As shown in Fig. 3, the bit error rate (BER) performance of the conventional (1x1)-system is very close to the case of a Rayleigh fading channel ($\nu = 1$). By means of the Alamouti scheme with two Tx and one Rx antenna, a significant performance gain is accomplished (6 dB at a BER of $5 \cdot 10^{-3}$). Utilization of a second Rx antenna yields further significant gain. At the same BER, the overall gain w.r.t. the (1x1)-system is 9 dB, where MRC of the two received signals was applied (see Section IV).

In the short distance scenario, there is no diversity to be gained. The Alamouti scheme therefore has the same performance as the (1x1)-system.

IV. Orthogonality Loss Due to Frequency Offsets

The Alamouti STBC was designed for quasi-static flat fading channels. In the following, it is shown that the orthogonal properties of the Alamouti STBC are lost given frequency offsets in the transmitter and/or the receiver, even if a modified receiver with perfect knowledge of all frequency offsets is employed. This orthogonality loss will cause a performance degradation. Similar considerations can be found in [8], where it is shown

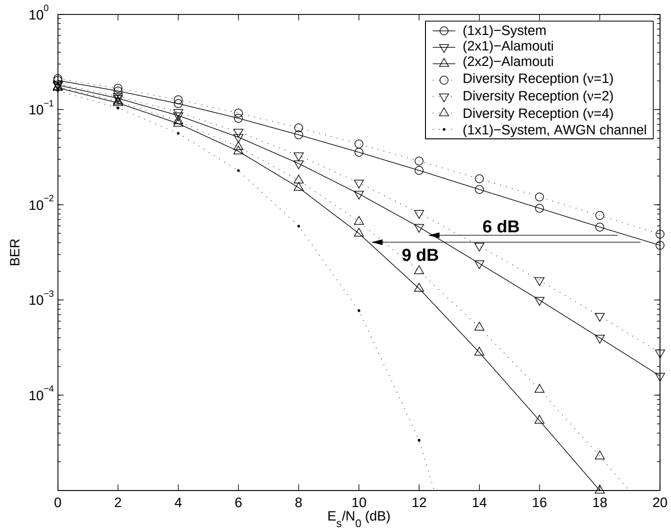

Fig. 3. Performance improvements for the long distance scenario.

that the orthogonal properties of the Alamouti STBC are lost in the case of non-perfect channel estimation as well as in the presence of fast fading or frequency-selective fading.

In the sequel, a quasi-static flat fading channel is assumed. In this case, each transmission path from Tx antenna i $(i=1,2)$ to Rx antenna j $(j=1,2)$ can be modeled by means of a complex-valued channel coefficient h_{ij} (effective memory length of the discrete-time channel model $L=0$), which is constant over the duration of an entire data block. It is assumed that the receiver has perfect knowledge of the channel coefficients at the beginning of each data block. For the time being, a single data block is considered.

A. Ideal Local Oscillators

First, it is assumed that all LOs are ideal, i.e., $\Delta f_{\mathrm{t}i}=0$ $(i=1,2)$ and $\Delta f_{\mathrm{r}j}=0$ $(j=1,2)$. Taking into account the space-time mapping according to the Alamouti matrix $\mathbf{A}$, the received symbols $y[k]$ and $y[k+1]$ are given by the following matrix equation [20, Ch. 7.3.2] (one Rx antenna is assumed) :

$$\underbrace{\begin{bmatrix} y[k] \\ y^*[k+1] \end{bmatrix}}_{\mathbf{y}[k]} = c\cdot \underbrace{\begin{bmatrix} h_{11} & -h_{21} \\ h_{21}^* & h_{11}^* \end{bmatrix}}_{\mathbf{H}} \underbrace{\begin{bmatrix} x[k] \\ x^*[k+1] \end{bmatrix}}_{\mathbf{x}[k]} + \underbrace{\begin{bmatrix} n[k] \\ n^*[k+1] \end{bmatrix}}_{\mathbf{n}[k]}, \qquad (2)$$

where $c>0$ is an arbitrary real-valued normalization factor[4] and $n[k]$ and $n[k+1]$ denote samples of a complex additive white Gaussian noise (AWGN) process with variance σ_{n}^2, taken at time index k and $k+1$, respectively. The channel matrix $\mathbf{H}$ is orthogonal, which is due to the orthogonality of the Alamouti matrix $\mathbf{A}$.

[4]For a fair comparison with the conventional (1x1)-system, the overall transmitted power should be normalized with respect to the number of Tx antennas used, i.e., c should be chosen as $c \doteq 1/\sqrt{2}$.

Maximum-likelihood (ML) detection of the symbols $x[k]$ and $x[k+1]$ can simply be performed by means of the matrix-vector multiplication $\mathbf{H}^{\mathrm{H}}\mathbf{y}[k]$ [15]. In this context, the orthogonality of $\mathbf{H}$ leads to a decoupling of $x[k]$ and $x[k+1]$ in terms of *independent* (soft) estimates $\hat{x}[k]$ and $\hat{x}[k+1]$:

$$\hat{\mathbf{x}}[k] = \mathbf{H}^{\mathrm{H}}\mathbf{y}[k] = c\,\mathbf{H}^{\mathrm{H}}\mathbf{H}\,\mathbf{x}[k] + \bar{\mathbf{n}}[k], \quad \text{where}$$

$$\hat{\mathbf{x}}[k] = \begin{bmatrix} \hat{x}[k] \\ \hat{x}^*[k+1] \end{bmatrix}, \quad \bar{\mathbf{n}}[k] = \mathbf{H}^{\mathrm{H}}\mathbf{n}[k] \quad \text{and}$$

$$\mathbf{H}^{\mathrm{H}}\mathbf{H} = \underbrace{\left(|h_{11}|^2 + |h_{21}|^2\right)}_{\doteq\,\Theta}\,\mathbf{I}_2\,. \qquad (3)$$

Note that due to the diagonal structure of $\mathbf{H}^{\mathrm{H}}\mathbf{H}$, the desired symbols are always combined in a constructive way, because they are multiplied by a sum of absolute terms. The noise, however, is combined incoherently (matrix $\mathbf{H}^{\mathrm{H}}$), which leads to a diversity gain over the conventional (1x1)-system. The modified noise term is still white (and Gaussian) [15] since the autocorrelation matrix of $\bar{\mathbf{n}}[k]$ is diagonal:

$$\mathbf{R}_{\bar{\mathbf{n}}\bar{\mathbf{n}}} \doteq \mathrm{E}\left\{\bar{\mathbf{n}}[k]\,\bar{\mathbf{n}}[k]^{\mathrm{H}}\right\} = \Theta\,\sigma_{\mathrm{n}}^2 \cdot \mathbf{I}_2, \qquad (4)$$

where $\mathrm{E}\{.\}$ denotes expectation. Clearly, ML detection of the data symbols $x[k]$ and $x[k+1]$ according to (3) still works if one of the Tx antennas fails, because this corresponds to the special case $h_{11}=0$ or $h_{21}=0$. However, a 3 dB loss in transmission power has to be taken into account.

If a second Rx antenna is used, the vectors and matrices in (2) are given by

$$\mathbf{y}[k] = \begin{bmatrix} y_1[k] \\ y_1^*[k+1] \\ y_2[k] \\ y_2^*[k+1] \end{bmatrix}, \qquad \mathbf{H} = \begin{bmatrix} h_{11} & -h_{21} \\ h_{21}^* & h_{11}^* \\ h_{12} & -h_{22} \\ h_{22}^* & h_{12}^* \end{bmatrix},$$

$$\mathbf{x}[k] = \begin{bmatrix} x[k] \\ x^*[k+1] \end{bmatrix}, \qquad \mathbf{n}[k] = \begin{bmatrix} n_1[k] \\ n_1^*[k+1] \\ n_2[k] \\ n_2^*[k+1] \end{bmatrix}, \qquad (5)$$

where $y_j[.]$ and $n_j[.]$ denote the received symbols and the noise samples at Rx antenna j, respectively $(j=1,2)$. The soft estimate $\hat{\mathbf{x}}[k]$ of $\mathbf{x}[k]$ is obtained as stated in (3), where now

$$\Theta = \left(|h_{11}|^2 + |h_{12}|^2 + |h_{21}|^2 + |h_{22}|^2\right), \qquad (6)$$

i.e., MRC of the two received signals is performed.

B. Frequency Offsets Unknown at the Receiver

Now, frequency offsets $\Delta f_{\mathrm{t}i}$ $(i=1,2)$ and $\Delta f_{\mathrm{r}j}$ $(j=1,2)$ occurring at the transmitter and the receiver, respectively, shall be taken into account. The frequency offsets $\Delta f_{\mathrm{t}1}$ and $\Delta f_{\mathrm{t}2}$ are typically different due to the resilient Tx structure (the same holds for $\Delta f_{\mathrm{r}1}$ and $\Delta f_{\mathrm{r}2}$). In the transmitter, up-conversion of the transmission signal of Tx antenna i is performed by multiplying the baseband signal with $\exp[+\mathrm{i}\,2\pi(f_{\mathrm{c}}+\Delta f_{\mathrm{t}i})\,t]$ (cf.

Fig. 1), where t denotes the absolute time and $\mathrm{i} = \sqrt{-1}$. Down-conversion in the receiver is done by multiplying the received signal of Rx antenna j with $\exp[-\mathrm{i}\, 2\pi(f_\mathrm{c} + \Delta f_{\mathrm{r}j})\, t]$. Therefore, the channel coefficient associated with the transmission path from Tx antenna i to Rx antenna j can be modeled as

$$h_{ij} \exp[\mathrm{i}\, 2\pi \Delta f_{ij}\, kT] \doteq h_{ij} \exp[\mathrm{i}\, \varphi_{ij}[k]],$$

where T denotes the symbol duration and $\Delta f_{ij} \doteq \Delta f_{\mathrm{t}i} - \Delta f_{\mathrm{r}j}$. This leads to a modified channel matrix, which is now time-varying. If a single Rx antenna is used, one obtains

$$\tilde{\mathbf{H}}[k] = \left[\begin{array}{cc} h_{11} \cdot \mathrm{e}^{\mathrm{i}\varphi_{11}[k]} & -h_{21} \cdot \mathrm{e}^{\mathrm{i}\varphi_{21}[k]} \\ h_{21}^* \cdot \mathrm{e}^{-\mathrm{i}\varphi_{21}[k+1]} & h_{11}^* \cdot \mathrm{e}^{-\mathrm{i}\varphi_{11}[k+1]} \end{array} \right], \tag{7}$$

and in the case of a second Rx antenna

$$\tilde{\mathbf{H}}[k] = \left[\begin{array}{cc} h_{11} \cdot \mathrm{e}^{\mathrm{i}\varphi_{11}[k]} & -h_{21} \cdot \mathrm{e}^{\mathrm{i}\varphi_{21}[k]} \\ h_{21}^* \cdot \mathrm{e}^{-\mathrm{i}\varphi_{21}[k+1]} & h_{11}^* \cdot \mathrm{e}^{-\mathrm{i}\varphi_{11}[k+1]} \\ h_{12} \cdot \mathrm{e}^{\mathrm{i}\varphi_{12}[k]} & -h_{22} \cdot \mathrm{e}^{\mathrm{i}\varphi_{22}[k]} \\ h_{22}^* \cdot \mathrm{e}^{-\mathrm{i}\varphi_{22}[k+1]} & h_{12}^* \cdot \mathrm{e}^{-\mathrm{i}\varphi_{12}[k+1]} \end{array} \right]. \tag{8}$$

Suppose that for $k=0$, the channel coefficients h_{ij} are perfectly known at the receiver, but the frequency offsets are not taken into account. Then the receiver will use matrix $\mathbf{H}$ instead of $\tilde{\mathbf{H}}[k]$ in order to perform symbol detection according to (3). Then,

$$\hat{\mathbf{x}}[k] = c\, \mathbf{H}^\mathrm{H} \tilde{\mathbf{H}}[k]\, \mathbf{x}[k] \;+\; \bar{\mathbf{n}}[k]. \tag{9}$$

The noise vector $\bar{\mathbf{n}}[k]$ is the same as in (3). However, the matrix product $\mathbf{H}^\mathrm{H}\tilde{\mathbf{H}}[k]$ is no longer a diagonal matrix:

$$\mathbf{H}^\mathrm{H}\tilde{\mathbf{H}}[k] \doteq \left[\begin{array}{cc} \chi_1[k] & \nu_1[k] \\ \nu_2[k] & \chi_2[k] \end{array} \right] \;\neq\; \text{const.} \cdot \mathbf{I}_2. \tag{10}$$

In the case of a single Rx antenna, one obtains

$$\begin{aligned} \chi_1[k] &= |h_{11}|^2 \cdot \mathrm{e}^{\mathrm{i}\varphi_{11}[k]} + |h_{21}|^2 \cdot \mathrm{e}^{-\mathrm{i}\varphi_{21}[k+1]} \\ \chi_2[k] &= |h_{11}|^2 \cdot \mathrm{e}^{-\mathrm{i}\varphi_{11}[k+1]} + |h_{21}|^2 \cdot \mathrm{e}^{\mathrm{i}\varphi_{21}[k]} \end{aligned} \tag{11}$$

$$\begin{aligned} \nu_1[k] &= h_{11}^* h_{21} \left(\mathrm{e}^{-\mathrm{i}\varphi_{11}[k+1]} - \mathrm{e}^{\mathrm{i}\varphi_{21}[k]} \right) \\ \nu_2[k] &= h_{11} h_{21}^* \left(\mathrm{e}^{-\mathrm{i}\varphi_{21}[k+1]} - \mathrm{e}^{\mathrm{i}\varphi_{11}[k]} \right). \end{aligned}$$

The corresponding expressions for the case of two Rx antennas are given in the Appendix.

This loss of orthogonality means that the desired symbols $x[k]$ and $x[k+1]$ are not necessarily combined in a constructive way anymore, because now the absolute terms in the diagonal elements of $\mathbf{H}^\mathrm{H}\tilde{\mathbf{H}}[k]$ have erroneous phase-offsets. Apart from this, $x[k]$ and $x[k+1]$ are weighted by different factors $\chi_1[k]$ and $\chi_2[k]$. The secondary diagonal elements $\nu_1[k]$ and $\nu_2[k]$ introduce an additional error term to the soft estimates $\hat{x}[k]$ and $\hat{x}[k+1]$ [5]. Note that (10) reduces to (3) if all frequency offsets Δf_{ij} are zero.

[5] Similar effects are caused in a cellular mobile radio system employing the Alamouti STBC if the channel is time-varying due to motion of the mobile station [8].

C. Frequency-Offset Estimates Available at the Receiver

In the sequel, it is assumed that estimates $\Delta\hat{f}_{ij}$ of the frequency offsets Δf_{ij} are available at the receiver, where

$$\Delta\hat{f}_{ij} \doteq \Delta f_{ij} + \epsilon_{ij}. \tag{12}$$

In the case of a single Rx antenna, the above receiver may then be modified such that the matrix

$$\tilde{\mathbf{H}}_\epsilon[k] \doteq \left[\begin{array}{cc} h_{11} \cdot \mathrm{e}^{\mathrm{i}\hat{\varphi}_{11}[k]} & -h_{21} \cdot \mathrm{e}^{\mathrm{i}\hat{\varphi}_{21}[k]} \\ h_{21}^* \cdot \mathrm{e}^{-\mathrm{i}\hat{\varphi}_{21}[k+1]} & h_{11}^* \cdot \mathrm{e}^{-\mathrm{i}\hat{\varphi}_{11}[k+1]} \end{array} \right], \tag{13}$$

is used in order to perform the symbol detection according to (3), where $\hat{\varphi}_{ij}[k] = 2\pi\Delta\hat{f}_{ij}\, kT = 2\pi(\Delta f_{ij} + \epsilon_{ij})\, kT$, and in the case of two Rx antennas the matrix

$$\tilde{\mathbf{H}}_\epsilon[k] = \left[\begin{array}{cc} h_{11} \cdot \mathrm{e}^{\mathrm{i}\hat{\varphi}_{11}[k]} & -h_{21} \cdot \mathrm{e}^{\mathrm{i}\hat{\varphi}_{21}[k]} \\ h_{21}^* \cdot \mathrm{e}^{-\mathrm{i}\hat{\varphi}_{21}[k+1]} & h_{11}^* \cdot \mathrm{e}^{-\mathrm{i}\hat{\varphi}_{11}[k+1]} \\ h_{12} \cdot \mathrm{e}^{\mathrm{i}\hat{\varphi}_{12}[k]} & -h_{22} \cdot \mathrm{e}^{\mathrm{i}\hat{\varphi}_{22}[k]} \\ h_{22}^* \cdot \mathrm{e}^{-\mathrm{i}\hat{\varphi}_{22}[k+1]} & h_{12}^* \cdot \mathrm{e}^{-\mathrm{i}\hat{\varphi}_{12}[k+1]} \end{array} \right]. \tag{14}$$

In this case,

$$\hat{\mathbf{x}}[k] = c\, \tilde{\mathbf{H}}_\epsilon^\mathrm{H}[k]\, \tilde{\mathbf{H}}[k]\, \mathbf{x}[k] \;+\; \check{\mathbf{n}}[k], \tag{15}$$

where

$$\tilde{\mathbf{H}}_\epsilon^\mathrm{H}[k]\, \tilde{\mathbf{H}}[k] \doteq \left[\begin{array}{cc} \kappa_1[k] & \psi_1[k] \\ \psi_2[k] & \kappa_2[k] \end{array} \right] \tag{16}$$

and

$$\check{\mathbf{n}}[k] = \tilde{\mathbf{H}}_\epsilon^\mathrm{H}[k]\, \mathbf{n}[k]. \tag{17}$$

In the case of a single Rx antenna, one obtains

$$\begin{aligned} \kappa_1[k] &= |h_{11}|^2 \cdot \mathrm{e}^{-\mathrm{i}2\pi\epsilon_{11}kT} + |h_{21}|^2 \cdot \mathrm{e}^{\mathrm{i}2\pi\epsilon_{21}(k+1)T} \\ \kappa_2[k] &= |h_{11}|^2 \cdot \mathrm{e}^{\mathrm{i}2\pi\epsilon_{11}(k+1)T} + |h_{21}|^2 \cdot \mathrm{e}^{-\mathrm{i}2\pi\epsilon_{21}kT} \end{aligned} \tag{18}$$

$$\begin{aligned} \psi_1[k] &= h_{11}^* h_{21} \left(\mathrm{e}^{\mathrm{i}(\hat{\varphi}_{21}[k+1] - \varphi_{11}[k+1])} - \mathrm{e}^{\mathrm{i}(\varphi_{21}[k] - \hat{\varphi}_{11}[k])} \right) \\ \psi_2[k] &= h_{11} h_{21}^* \left(\mathrm{e}^{\mathrm{i}(\hat{\varphi}_{11}[k+1] - \varphi_{21}[k+1])} - \mathrm{e}^{\mathrm{i}(\varphi_{11}[k] - \hat{\varphi}_{21}[k])} \right). \end{aligned}$$

The expressions for the case of two Rx antennas are given in the Appendix.

It is important to note that the modified noise term $\check{\mathbf{n}}[k]$ is *not* white anymore, since its auto-correlation matrix is given by

$$\mathbf{R}_{\check{\mathbf{n}}\check{\mathbf{n}}} = \sigma_\mathrm{n}^2 \cdot \tilde{\mathbf{H}}_\epsilon^\mathrm{H}[k]\, \tilde{\mathbf{H}}_\epsilon[k] = \sigma_\mathrm{n}^2 \cdot \left[\begin{array}{cc} \Theta & \tilde{\psi}_1[k] \\ \tilde{\psi}_2[k] & \Theta \end{array} \right], \tag{19}$$

where $\tilde{\psi}_1[k]$ and $\tilde{\psi}_2[k]$ are in principle given by the expressions for $\psi_1[k]$ and $\psi_2[k]$, with the only difference that in $\tilde{\psi}_1[k]$ and $\tilde{\psi}_2[k]$ all phase-terms $\varphi_{ij}[.]$ are estimates. For example, given one Rx antenna,

$$\tilde{\psi}_1[k] = h_{11}^* h_{21} \left(\mathrm{e}^{\mathrm{i}(\hat{\varphi}_{21}[k+1] - \hat{\varphi}_{11}[k+1])} - \mathrm{e}^{\mathrm{i}(\hat{\varphi}_{21}[k] - \hat{\varphi}_{11}[k])} \right).$$

If all frequency offsets involved are perfectly known at the receiver, i.e., $\epsilon_{ij} \to 0$ for all i, j, then one obtains

$$\lim_{\epsilon_{ij} \to 0} \tilde{\mathbf{H}}_\epsilon^\mathrm{H}[k]\, \tilde{\mathbf{H}}[k] = \tilde{\mathbf{H}}^\mathrm{H}[k]\, \tilde{\mathbf{H}}[k] = \left[\begin{array}{cc} \Theta & \xi[k] \\ \xi^*[k] & \Theta \end{array} \right], \tag{20}$$

where in the case of a single Rx antenna

$$\xi[k] = h_{11}^* h_{21} \left(\mathrm{e}^{\mathrm{i}(\varphi_{21}[k+1]-\varphi_{11}[k+1])} - \mathrm{e}^{\mathrm{i}(\varphi_{21}[k]-\varphi_{11}[k])} \right). \quad (21)$$

For the case of two Rx antennas, see the Appendix.

Note that, although all frequency offsets are perfectly known at the receiver, the soft estimate $\hat{\mathbf{x}}[k]$ is still erroneous if $\Delta f_{11} \neq \Delta f_{21}$. Also, the noise term $\lim_{\epsilon_{ij}\to 0} \check{\mathbf{n}}[k]$ is not white, since

$$\mathbf{R}_{\check{\mathbf{n}}\check{\mathbf{n}}} = \sigma_{\mathrm{n}}^2 \cdot \tilde{\mathbf{H}}^{\mathrm{H}}[k]\, \tilde{\mathbf{H}}[k] \quad (22)$$

is not diagonal (cf. (20)).

D. Example for the Influence of the Frequency Offsets

In the following, the influence of the frequency offsets on the soft estimate $\hat{\mathbf{x}}[k]$ of the data symbol vector $\mathbf{x}[k]$ shall be illustrated for the case of one Rx antenna. The nominal carrier frequency is assumed to be $f_{\mathrm{c}} = 20$ GHz and the frequency offsets[6] are $\Delta f_{11} = 15$ppm and $\Delta f_{21} = -6$ppm w.r.t. f_{c}. The symbol duration T is set to $0.1\,\mu$s, QPSK mapping ($M = 4$) is assumed, and a block length of $N = 100$ symbols.

Fig. 4 a)-c) shows the influence of the frequency offsets for several cases. For a constant channel matrix with $h_{11} = h_{21} = 1$, and even time indices, the soft estimates $\hat{x}[k+2n]$ are depicted within the complex plane (n integer), for $E_s/N_0 \to \infty$. The corresponding symbol error probabilities are as well depicted. At each even time index, the same symbol $x[k+2n] = \exp[\mathrm{i}\,\pi/4]$ is transmitted. In Fig. 4 a) and b), the frequency offsets are unknown at the receiver. In Fig. 4 a), at each odd time index the same symbol $x[k+2n+1] = \exp[\mathrm{i}\,\pi/4]$ is transmitted, which yields a regular structure within the complex plane. As opposed to this, in Fig. 4 b) the symbols $x[k+2n+1]$ transmitted at odd time indices are chosen randomly. Obviously, the frequency offsets severely affect the quality of the soft estimates. In Fig. 4 c), the frequency offsets are perfectly known at the receiver. In turn, the symbols $x[k+2n+1]$ transmitted at odd time indices are chosen randomly. Clearly, the soft estimates $\hat{x}[k+2n]$ are significantly improved if the frequency offsets are perfectly known at the receiver (cf. Fig. 4 b) and c)). However, they are still erroneous (cf. (20)).

V. Bit Error Probability

In this section, analytical expressions for the bit error probability are derived, for the example of QPSK ($M = 4$) and a quasi-static frequency-flat fading channel. To start with, a single data block shall be considered in the following.

Let b_{1k} and b_{2k} denote the first and the second bit mapped on the quaternary symbol $x[k]$ ($\{b_{1k}b_{2k}\} \mapsto x[k]$) and let $\hat{x}[k]$ denote the corresponding soft estimate. Gray mapping of the bits is assumed according to

$$\begin{array}{ll} \{00\} \mapsto \exp[\mathrm{i}\,\pi/4] & \{01\} \mapsto \exp[\mathrm{i}\,3\pi/4] \\ \{11\} \mapsto \exp[\mathrm{i}\,5\pi/4] & \{10\} \mapsto \exp[\mathrm{i}\,7\pi/4]. \end{array}$$

[6]For state-of-the-art LOs, it is realistic to assume an absolute frequency offset $\leq$ 10ppm w.r.t. f_{c}. Therefore, Δf_{ij} may be assumed to be within $\pm$20ppm w.r.t. f_{c} for all i, j.

Let $d_{\mathrm{Re}}[k] \doteq \mathrm{Re}\{\hat{x}[k]\}$ and $d_{\mathrm{Im}}[k] \doteq \mathrm{Im}\{\hat{x}[k]\}$ denote the real and the imaginary part of $\hat{x}[k]$ for $E_s/N_0 \to \infty$, respectively. The bit error probability for b_{1k} is given by [19, Ch. 5.2]

$$P_{\mathrm{b}1}[k] = \mathrm{Q}\left(\sqrt{2\, \frac{d_{\mathrm{Im}}^2[k]}{\Theta}\, \frac{E_s}{N_0}} \right), \quad (23)$$

if the imaginary parts of $x[k]$ and $\hat{x}[k]$ have equal signs, otherwise by

$$P_{\mathrm{b}1}[k] = \bar{\mathrm{Q}}\left(\sqrt{2\, \frac{d_{\mathrm{Im}}^2[k]}{\Theta}\, \frac{E_s}{N_0}} \right), \quad (24)$$

where

$$\mathrm{Q}(x) = \frac{1}{\sqrt{2\pi}} \int_x^\infty \exp\left(\frac{-\zeta^2}{2} \right) \mathrm{d}\zeta \quad (25)$$

and $\bar{\mathrm{Q}}(x) = 1 - \mathrm{Q}(x)$. In the case of two Rx antennas, E_s/N_0 in (23) and (24) is per Rx antenna. Likewise, the bit error probability for b_{2k} is given by

$$P_{\mathrm{b}2}[k] = \mathrm{Q}\left(\sqrt{2\, \frac{d_{\mathrm{Re}}^2[k]}{\Theta}\, \frac{E_s}{N_0}} \right), \quad (26)$$

if the real parts of $x[k]$ and $\hat{x}[k]$ have equal signs, otherwise by

$$P_{\mathrm{b}2}[k] = \bar{\mathrm{Q}}\left(\sqrt{2\, \frac{d_{\mathrm{Re}}^2[k]}{\Theta}\, \frac{E_s}{N_0}} \right). \quad (27)$$

In the following, analytical expressions for the distances $d_{\mathrm{Re}}[k]$ and $d_{\mathrm{Im}}[k]$ are developed for different cases. In the case of ideal LOs (Section IV-A), one obtains

$$d_{\mathrm{Re}}[k] = c\,\Theta\,\mathrm{Re}\{x[k]\}, \;\; d_{\mathrm{Im}}[k] = c\,\Theta\,\mathrm{Im}\{x[k]\}. \quad (28)$$

In the case of non-ideal LOs, one has to distinguish between even and odd time indices. If the frequency offsets are unknown at the receiver (Section IV-B), $d_{\mathrm{Re}}[.]$ and $d_{\mathrm{Im}}[.]$ are given by

$$\begin{aligned} d_{\mathrm{Re}}[k] &= c\,\mathrm{Re}\{\, \chi_1[k]\, x[k] + \nu_1[k]\, x^*[k+1] \,\} \\ d_{\mathrm{Im}}[k] &= c\,\mathrm{Im}\{\, \chi_1[k]\, x[k] + \nu_1[k]\, x^*[k+1] \,\} \quad (29) \\ d_{\mathrm{Re}}[k+1] &= c\,\mathrm{Re}\{\, \nu_2^*[k]\, x^*[k] + \chi_2^*[k]\, x[k+1] \,\} \\ d_{\mathrm{Im}}[k+1] &= c\,\mathrm{Im}\{\, \nu_2^*[k]\, x^*[k] + \chi_2^*[k]\, x[k+1] \,\}. \end{aligned}$$

If the frequency offsets are perfectly known at the receiver (Section IV-C), one finds that

$$\begin{aligned} d_{\mathrm{Re}}[k] &= c\,\mathrm{Re}\{\, \Theta\, x[k] + \xi[k]\, x^*[k+1] \,\} \\ d_{\mathrm{Im}}[k] &= c\,\mathrm{Im}\{\, \Theta\, x[k] + \xi[k]\, x^*[k+1] \,\} \quad (30) \\ d_{\mathrm{Re}}[k+1] &= c\,\mathrm{Re}\{\, \xi[k]\, x^*[k] + \Theta\, x[k+1] \,\} \\ d_{\mathrm{Im}}[k+1] &= c\,\mathrm{Im}\{\, \xi[k]\, x^*[k] + \Theta\, x[k+1] \,\}. \end{aligned}$$

The expectation of the bit error probability $P_{\mathrm{b}i}[k]$ ($i = 1, 2$) with respect to the channel coefficients is given by

$$\bar{P}_{\mathrm{b}i}[k] = \int p_h(\mathbf{h})\; P_{\mathrm{b}i}[k]\; \mathrm{d}\mathbf{h}, \quad (31)$$

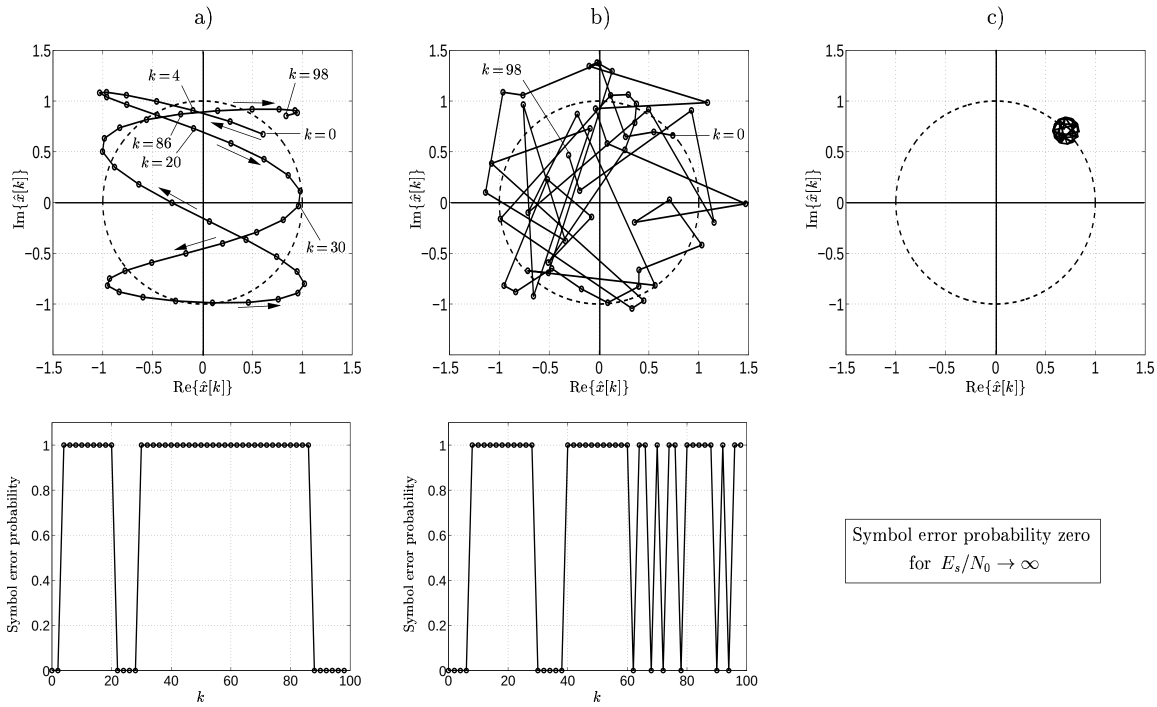

Fig. 4. Influence of the frequency offsets for different cases: Soft estimates $\hat{x}[k+2n]$ within the complex plane (n integer) and corresponding symbol error probabilities ($\Delta f_{11} = 15$ppm, $\Delta f_{21} = -6$ppm w.r.t. $f_c = 20$ GHz, $x[k+2n] = \exp[\mathrm{i}\,\pi/4]$ for each even time index, $E_s/N_0 \to \infty$) a) frequency offsets unknown at the receiver, same symbol $x[k+2n+1] = \exp[\mathrm{i}\,\pi/4]$ transmitted at each odd time index b) frequency offsets unknown at the receiver, symbols $x[k+2n+1]$ chosen randomly c) frequency offsets perfectly known at the receiver, symbols $x[k+2n+1]$ chosen randomly.

where $p_h(\mathbf{h})$ denotes the joint pdf of the channel coefficients. The integral is over all possible realizations of $\mathbf{h}$.The overall average bit error probability, given blocks of N QPSK symbols, results as

$$\bar{P}_\mathrm{b} = \frac{1}{2N} \sum_{k=1}^{N} \bar{P}_{\mathrm{b}1}[k] + \bar{P}_{\mathrm{b}2}[k] \,. \tag{32}$$

VI. Simulation Results

In the following, the performance loss shall be illustrated which occurs in the case of perfect and non-perfect knowledge of the frequency-offsets at the receiver. The simulation setup corresponds to that in Section III-B. The simulation results are restricted to the case of a single Rx antenna. For the quasi-static frequency-flat Rician fading channel model, a Rice factor of $K = 0$ dB was assumed. The simulation results were obtained by means of Monte-Carlo simulations over 10.000 blocks, where each block contained $N = 100$ QPSK symbols. At the receiver, the channel coefficients were perfectly known at the beginning of each block, i.e., the observed performance degradations are solely due to the time-varying phase caused by the frequency offsets. The symbol duration was chosen as $T = 0.1\,\mu$s.

Fig. 5 shows the average BERs as a function of E_s/N_0 resulting for several cases, given frequency offsets $\Delta f_{11} = 15$ppm and $\Delta f_{21} = -6$ppm w.r.t. the carrier frequency $f_c = 20$ GHz. The BER curves for the (1x1)-system and for the Alamouti STBC in the case of ideal oscillators are included as a reference (solid lines). The dashed lines represent the extreme cases of unknown frequency offsets at the receiver and perfect knowledge of the frequency offsets. The corresponding analytical curves obtained on the basis of Section V are as well included. The average bit error probability according to (31) and (32) was computed by averaging over 10.000 realizations of the channel coefficients. As can be seen, simulative and analytical curves are in good accordance. For perfect knowledge of the frequency offsets at the receiver, the BER performance is very close to the case of ideal oscillators despite the loss of orthogonality, i.e., the influence of the secondary diagonal elements in (20) is rather small. When the frequency offsets are unknown, however, a huge average BER of about 0.5 results for all SNR values. Finally, the dotted lines represent the case where non-perfect estimates of the frequency offsets are available at the receiver. If only a single frequency-offset estimate is noisy, the effect is rather small. Given an error of +5 per cent concerning the estimate of the first frequency offset, the performance loss with respect to the case of perfect knowledge is less than 1 dB at a BER of 10^{-2}. However, if both frequency-offset estimates are subject to an error of +5 per cent, a significant performance degradation results.

VII. Summary and Conclusions

In this paper, the novel possible application of the Alamouti scheme as a switchless alternative in resilient microwave radio links has been investigated. For the application example of a wireless interconnection of two base stations within a cellular mobile radio network, it has been demonstrated that significant diversity gains are accomplished under realistic assumptions.

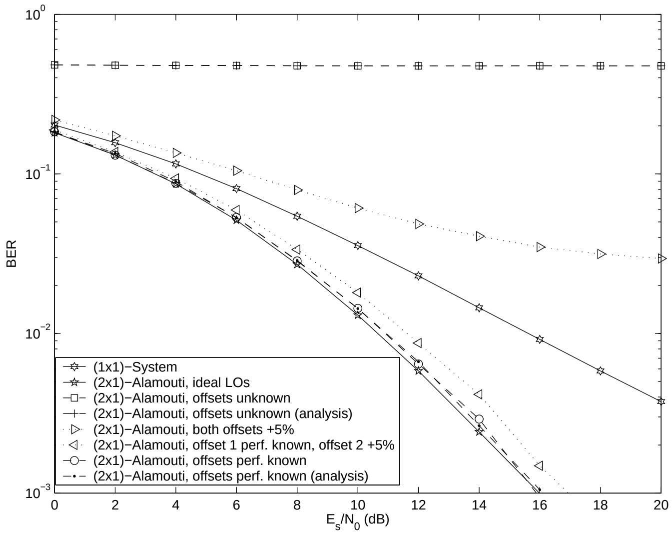

Fig. 5. Simulative and analytical results illustrating the performance loss which occurs in the case of perfect and non-perfect knowledge of the frequency-offsets at the receiver (frequency offsets $\Delta f_{11} = 15$ppm and $\Delta f_{21} = -6$ppm w.r.t. the carrier frequency $f_c = 20$ GHz).

The influence of frequency offsets has been investigated. Due to the resilient Tx/Rx structure, two different frequency offsets typically occur at either Tx/Rx antenna. It has been shown that these frequency offsets severely affect the quality of the soft estimates of the transmitted data symbols at the receiver. The soft estimates can be significantly improved if the receiver has perfect knowledge of the frequency offsets. However, a complete compensation for the influence of the frequency offsets is still not accomplished.

APPENDIX

For the case of two Rx antennas, one obtains the following expressions for the matrix entries $\chi_{1,2}[k]$ and $\nu_{1,2}[k]$ in (10):

$$\begin{aligned}
\chi_1[k] &= |h_{11}|^2 \cdot e^{i\varphi_{11}[k]} + |h_{21}|^2 \cdot e^{-i\varphi_{21}[k+1]} \\
&+ |h_{12}|^2 \cdot e^{i\varphi_{12}[k]} + |h_{22}|^2 \cdot e^{-i\varphi_{22}[k+1]} \\
\chi_2[k] &= |h_{11}|^2 \cdot e^{-i\varphi_{11}[k+1]} + |h_{21}|^2 \cdot e^{i\varphi_{21}[k]} \\
&+ |h_{12}|^2 \cdot e^{-i\varphi_{12}[k+1]} + |h_{22}|^2 \cdot e^{i\varphi_{22}[k]} \\
\nu_1[k] &= h_{11}^* h_{21} \left(e^{-i\varphi_{11}[k+1]} - e^{i\varphi_{21}[k]}\right) \\
&+ h_{12}^* h_{22} \left(e^{-i\varphi_{12}[k+1]} - e^{i\varphi_{22}[k]}\right) \\
\nu_2[k] &= h_{11} h_{21}^* \left(e^{-i\varphi_{21}[k+1]} - e^{i\varphi_{11}[k]}\right) \\
&+ h_{12} h_{22}^* \left(e^{-i\varphi_{22}[k+1]} - e^{i\varphi_{12}[k]}\right).
\end{aligned}$$

For the matrix entries $\kappa_{1,2}[k]$ and $\psi_{1,2}[k]$ in (16), one finds

$$\begin{aligned}
\kappa_1[k] &= |h_{11}|^2 \cdot e^{-i2\pi\epsilon_{11}kT} + |h_{21}|^2 \cdot e^{i2\pi\epsilon_{21}(k+1)T} \\
&+ |h_{12}|^2 \cdot e^{-i2\pi\epsilon_{12}kT} + |h_{22}|^2 \cdot e^{i2\pi\epsilon_{22}(k+1)T} \\
\kappa_2[k] &= |h_{11}|^2 \cdot e^{i2\pi\epsilon_{11}(k+1)T} + |h_{21}|^2 \cdot e^{-i2\pi\epsilon_{21}kT} \\
&+ |h_{12}|^2 \cdot e^{i2\pi\epsilon_{12}(k+1)T} + |h_{22}|^2 \cdot e^{-i2\pi\epsilon_{22}kT}
\end{aligned}$$

$$\begin{aligned}
\psi_1[k] &= h_{11}^* h_{21} \left(e^{i(\hat\varphi_{21}[k+1]-\varphi_{11}[k+1])} - e^{i(\varphi_{21}[k]-\hat\varphi_{11}[k])}\right) \\
&+ h_{12}^* h_{22} \left(e^{i(\hat\varphi_{22}[k+1]-\varphi_{12}[k+1])} - e^{i(\varphi_{22}[k]-\hat\varphi_{12}[k])}\right) \\
\psi_2[k] &= h_{11} h_{21}^* \left(e^{i(\hat\varphi_{11}[k+1]-\varphi_{21}[k+1])} - e^{i(\varphi_{11}[k]-\hat\varphi_{21}[k])}\right) \\
&+ h_{12} h_{22}^* \left(e^{i(\hat\varphi_{12}[k+1]-\varphi_{22}[k+1])} - e^{i(\varphi_{12}[k]-\hat\varphi_{22}[k])}\right).
\end{aligned}$$

The matrix entry $\xi[k]$ in (20) is given by

$$\begin{aligned}
\xi[k] &= h_{11}^* h_{21} \left(e^{i(\varphi_{21}[k+1]-\varphi_{11}[k+1])} - e^{i(\varphi_{21}[k]-\varphi_{11}[k])}\right) \\
&+ h_{12}^* h_{22} \left(e^{i(\varphi_{22}[k+1]-\varphi_{12}[k+1])} - e^{i(\varphi_{22}[k]-\varphi_{12}[k])}\right).
\end{aligned}$$

REFERENCES

[1] D. Gesbert, M. Shafi, D. Shiu, P. J. Smith, and A. Naguib, "From theory to practice: An overview of MIMO space-time coded wireless systems," *IEEE J. Select. Areas Commun.*, vol. 21, no. 3, pp. 281-302, Apr. 2003.

[2] E. Telatar, "Capacity of multi-antenna Gaussian channels," *Eur. Trans. Commun.*, vol. 10, no. 6, pp. 585-595, Nov.-Dec. 1999.

[3] G. J. Foschini and M. J. Gans, "On limits of wireless communications in a fading environment when using multiple antennas," *Wireless Pers. Commun.*, vol. 6, no. 3, pp. 311-335, Mar. 1998.

[4] G. J. Foschini, "Layered space-time architecture for wireless communication in a fading environment when using multi-element antennas," *Bell Labs Tech. J.*, pp. 41-59, Autumn 1996.

[5] A. F. Naguib, V. Tarokh, N. Seshadri, and A. R. Calderbank, "A space-time coding modem for high-data-rate wireless communications," *IEEE J. Select. Areas Commun.*, vol. 16, no. 8, pp. 1459-1478, Oct. 1998.

[6] A. M. Tehrani, R. Negi, and J. Cioffi, "Space-time coding over a code division multiple access system," in *Proc. Wireless Commun. and Networking Conf. (WCNC)*, 1999, pp. 134-138.

[7] H. Boelcskei and A. J. Paulraj, "Space-frequency coded broadband OFDM systems," in *Proc. Wireless Commun. and Networking Conf. (WCNC)*, 2000, pp. 1-6.

[8] J. Mietzner, P. A. Hoeher, and M. Sandell, "Compatible improvement of the GSM/EDGE system by means of space-time coding techniques," *IEEE Trans. Wireless Commun.*, vol. 2, no. 4, pp. 690-702, Jul. 2003.

[9] V. Tarokh, N. Seshadri, and A. R. Calderbank, "Space-time codes for high data rate wireless communication: Performance criterion and code construction," *IEEE Trans. Inform. Theory*, vol. 44, no. 2, pp. 744-765, Mar. 1998.

[10] V. Tarokh, A. Naguib, N. Seshadri, and A. R. Calderbank, "Space-time codes for high data rate wireless communication: Performance criteria in the presence of channel estimation errors, mobility, and multiple paths," *IEEE Trans. Commun.*, vol. 47, no. 2, pp. 199-207, Feb. 1999.

[11] V. Tarokh, H. Jafarkhani, and A. R. Calderbank, "Space-time block coding for wireless communications: Performance results," *IEEE J. Select. Areas Commun.*, vol. 17, no. 3, pp. 451-460, Mar. 1999.

[12] V. Tarokh, H. Jafarkhani, and A. R. Calderbank, "Space-time block codes from orthogonal designs," *IEEE Trans. Inform. Theory*, vol. 45, no. 5, pp. 1456-1467, June 1999.

[13] B. Hassibi and B. M. Hochwald, "High-rate codes that are linear in space and time," *IEEE Trans. Inform. Theory*, vol. 48, no. 7, pp. 1804-1824, Jul. 2002.

[14] J. Mietzner, M. Kautza, and P. A. Hoeher, "Application of the Alamouti scheme in resilient microwave radio links," *IEE Electron. Lett.*, vol. 39, no. 12, pp. 927-928, June 2003.

[15] S. M. Alamouti, "A simple transmit diversity technique for wireless communications," *IEEE J. Select. Areas Commun.*, vol. 16, no. 8, pp. 1451-1458, Oct. 1998.

[16] P. A. Anghel and M. Kaveh, "Relay assisted uplink communication over frequency-selective channels," in *Proc. IV IEEE Signal Processing Workshop on Signal Processing Adv. Wireless Commun. (SPAWC'03)*, 2003, paper no. 616.

[17] Nokia Networks, "Nokia FlexiHopper Microwave Radio," Product Overview C33513.21 H0, 2000.

[18] D. E. Kerr (Ed.), *Propagation of Short Radio Waves.* Reprinted, London: Peter Peregrinus, 1990.

[19] J. G. Proakis, *Digital Communications.* 4th ed., New York: McGraw-Hill, 2001.

[20] G. Bauch, *"Turbo-Entzerrung" und Sendeantennen-Diversity mit "Space-Time-Codes" im Mobilfunk.* PhD thesis, Department of Communications Engineering, Munich University of Technology, 2001.